JOURNAL OF THERMOPHYSICS AND HEAT TRANSFER
Vol. 9, No. 4, October–December 1995

# Viscous Dissipation in Non-Newtonian Flows: Implications for the Nusselt Number

R. M. Manglik*
*University of Cincinnati, Cincinnati, Ohio 45221-0072*
and
J. Prusa†
*Iowa State University, Ames, Iowa 50011-2160*

**This article considers the effects of viscous dissipation on convection heat transfer rates in thermally developing, power-law fluid flows in constant wall temperature tubes. The finite difference solution is based upon the use of asymptotic boundary-layer scales, and the results maintain high accuracy (errors $\leq$ 0.3% using 31 radial nodes) throughout the entrance region all the way to the fully developed condition. With viscous dissipation and hydrodynamically developed flow, the inlet temperature distribution is not uniform. Viscous dissipation effects are measured by the Brinkman number *Br* (ratio of viscous heating to convective heat transfer rates through the tube wall). Surprisingly, *Br* effects are found to be important primarily in a transition region between the inlet and fully developed flow condition. A very dramatic problem with the classical definition of Nusselt number *Nu* is also illuminated. Because *Nu* is based upon the bulk temperature, it exhibits local minima and may even show point discontinuities ($Nu \rightarrow \pm\infty$ as $z \rightarrow$ finite nonzero value). At the same axial locations, the wall temperature gradient remains well-behaved. This demonstrates that *Nu*, as usually defined, is an extremely poor measure of the local heat transfer rate in this region.**

## Nomenclature

$a$ = tube radius
$Br$, $Br^*$ = Brinkman number $(K/k \cdot \Delta T_i)(\bar{w}_m^{n+1}/a^{n-1})$, and modified Brinkman number ($Br^* = +Br$ if $Br > 0$, $Br^* = -Br$ if $Br < 0$), respectively
$Gz$ = Graetz number, $\pi/z$
$K$, $n$, $p$ = consistency, flow behavior index, and $[(n + 1)/n]$, respectively
$Nu$ = Nusselt number, Eqs. (25–28)
$Pe$ = Peclet number, $(a \cdot \bar{w}_m/\alpha)$
$Q$ = dimensionless convection heat transfer rate, Eq. (29)
$r$, $r_c$, $z$ = dimensionless boundary-layer radius, core radius, and axial coordinate, respectively
$\bar{r}$, $\bar{z}$ = dimensional radial and axial coordinates, respectively
$T^*$ = modified dimensionless temperature, Eq. (21)
$T_i^-$, $\Delta T_i$ = inlet or basic state wall temperature, and $(T_w - T_i^-)$, respectively
$\bar{T}$, $\bar{T}_m$ = dimensional temperature and bulk temperature, respectively (corresponding dimensionless variables are formed by removing overbars)
$\bar{T}_i$, $T_w$ = dimensional inlet or basic state temperature, and wall temperature, respectively (corresponding dimensionless variables are formed by removing overbars)
$\bar{w}$, $\bar{w}_m$ = dimensional axial and bulk velocities, respectively (corresponding dimensionless variables are formed by removing overbars)
$\alpha$, $c_p$, $k$, $\rho$ = thermal diffusivity, specific heat, thermal conductivity, and density of fluid, respectively
$\delta$, $\delta'$ = boundary-layer thickness, Eq. (19), and its axial derivative
$\eta$, $\tau_{rz}$ = apparent viscosity and shear stress, respectively
$\lambda$ = boundary-layer free parameter, Eq. (19)
$\tau$, $\tau^+$ = disturbance temperature, Eq. (15), and asymptotic disturbance temperature, Eq. (20), respectively

Received Aug. 12, 1994; revision received March 6, 1995; accepted for publication March 15, 1995. 

*Assistant Professor, Department of Mechanical, Industrial and Nuclear Engineering.
†Associate Professor, Department of Mechanical Engineering.

## Introduction

THE evaluation of heat transfer rates in thermally developing, laminar flows often involves highly viscous non-Newtonian, power-law fluids, for which viscous dissipation effects are important. This is especially the case, e.g., in thermal processing of plastics, polymeric melts and solutions, the production of emulsions and pastes, and the process heating or cooling of viscous gels. In many instances, the fluids are highly temperature sensitive, and the presence of large temperature variations induces product degradation; excessive viscous dissipation effects often aggravate such a situation. For several applications in the food, chemical, pharmaceutical, and process industries, the state of the end product leaving the heat exchanger is critical to the process efficiency and plant economics. This clearly warrants precise estimates of heat transfer rates in laminar flows with viscous dissipation under heating and cooling conditions, in order to ensure effective heat exchange in such applications.

Brinkman[1] first considered the problem of viscous dissipation in fully developed, laminar, isothermal flows of Newtonian fluids. Subsequently, theoretical solutions for thermally developing flows of Newtonian liquids in heated or cooled pipes with viscous dissipation effects have been reported in several studies.[2–5] In the much-cited work of Ou and Cheng,[3] a series solution, in terms of eigenvalues and eigenfunctions that satisfy the Strum–Liouville system, is presented. This solution, however, suffers from poor convergence in the deep thermal entrance region leading to inac-

curate results.[6,7] Numerical solutions to the extended Graetz problem[4,5] also do not give accurate results in the thermal entrance region. The inaccuracy primarily stems from an inadequate treatment of the singularity at the start of the thermally developing region in laminar pipe flows with uniform wall temperature. This difficulty is usually overcome by employing the Lévêque[8] solution. A computational extension of this approach by means of a singular perturbation has been reported by Prusa and Manglik[7] for the classical Graetz problem.

In laminar, non-Newtonian, power-law fluid flows in tubes with uniform wall temperature, the effect of viscous dissipation in the thermal entrance region has been considered in many earlier studies.[9-14] Shih and Tsou[10] have reported an extended Lévêque solution in the form of a power series by means of a coordinate perturbation method; up to fourth-order terms are presented, and the zero-order solution is the Lévêque solution for the generalized power-law fluid flows. Richardson[11] and Gottifredi and Flores[12] have presented alternate procedures for obtaining the extended Lévêque solution power series up to third-order terms. Gryglaszewski et al.,[13] and Lawal and Mujumdar[14] have solved the problem numerically using finite difference methods. In the former study, effects of temperature-dependent consistency index have also been included. As in the case of Newtonian fluid flows with viscous dissipation, with the exception of the Lévêque-type solutions, most others do not accurately describe the heat transfer rates in the deep thermal region; the extended Lévêque solutions, on the other hand, are not strictly valid far downstream in thermally developing flows.

The objective of this article is to present very accurate numerical solutions for the extended Graetz problem of viscous dissipation effects in laminar, power-law liquid flows in tubes with uniform wall temperature. Heat transfer results for wall heating and cooling are obtained for both shear thinning (pseudoplastic) and shear thickening (dilatant) fluids. The present study extends a previous work,[7] which demonstrated a finite difference method for obtaining highly accurate heat transfer rates for thermally developing, non-Newtonian flows for arbitrarily large Graetz number. The mathematical formulation is based upon the use of asymptotic, boundary-layer scales that are particularly appropriate for the deep entrance region. These scales require the use of boundary conditions based upon an isothermal core, i.e., a homogeneous temperature distribution at the start of the thermally developing (though hydrodynamically fully developed, large Prandtl number) flow. With the addition of viscous dissipation, however, the initial temperature is inhomogeneous. This inhomogeneity is removed by subtracting the initial profile from the developing profile and working only with the temperature disturbance; the disturbance itself is homogeneous at the inlet. The Brinkman number $Br$, which is the ratio of viscous heating to the heat transfer through the tube wall (impressed temperature difference), describes the effects of viscous dissipation, and, in the present model, $Br > 0$ for wall heating and $Br < 0$ for wall cooling. Very accurate results are presented for flow behavior index, $n < 1$ and $n > 1$ (as well as for $n = 1$, Newtonian fluid), and the effects of $Br$ are highlighted.

Finally, the accuracy of the results in the deep entrance region illuminates a major problem in the interpretation of Nusselt number $Nu$, which, in its conventional definition for pipe flow, is thought of as a measure of the convective heat transfer rate. When a fluid is cooled, the present results show that the local $Nu$ decreases from positive infinity at the inlet, reaches a minimum value, and then increases slightly to approach the fully developed value. This suggests that the heat transfer rate at the wall has a local minimum. Such is not the case. Inspection of the temperature gradient at the wall shows that it is a monotonically decreasing function of axial position. The local minimum in $Nu$ is thus an artifact of how it is defined, and in particular that it is a function of the fluid bulk temperature as well as the temperature gradient at the wall. Solutions for heating cases give even more absurd results for $Nu$. At some point from the inlet state, the fluid's bulk temperature will equal the wall temperature that is being imposed downstream of the inlet. At this point the local $Nu$ is undefined. Upstream of this point, it decreases from positive infinity at the inlet to negative infinity. Downstream of this point, the local $Nu$ decreases monotonically from positive infinity to its fully developed value at the zero $Gz$ limit. The temperature gradient at the wall is again a monotonically decreasing function of axial position. In the present example, the conventional $Nu$ is an extremely poor measure of the convection heat transfer rate, and an alternative dimensionless parameter is proposed.

## Mathematical Model

The physical model is a constant property, hydrodynamically fully developed, thermally developing, non-Newtonian laminar flow through a circular tube (see Fig. 1). A large $Pe$ number assumption is made so that axial conduction effects are ignored.

### Dimensional Formulation

A two-parameter Ostwald-de Waele, or power-law equation[15] is used to model the stress-strain relationship:

$$\tau_{rz} = \eta\left(\frac{\partial \bar{w}}{\partial \bar{r}}\right) \quad \text{and} \quad \eta = K\left(\frac{\partial \bar{w}}{\partial \bar{r}}\right)^{n-1} \tag{1}$$

where $K$ and $n$ are the consistency and flow behavior index, respectively. Expressions for the corresponding fully developed velocity field as well as the bulk velocity are well-known, and may be found in Prusa and Manglik.[7]

The energy equation, with viscous dissipation, takes on the form

$$w\frac{\partial \bar{T}}{\partial \bar{z}} = \frac{\alpha}{\bar{r}}\frac{\partial}{\partial \bar{r}}\left(\bar{r}\frac{\partial \bar{T}}{\partial \bar{r}}\right) + \frac{\eta}{\rho c_p}\left(\frac{\partial \bar{w}}{\partial \bar{r}}\right)^2 \tag{2}$$

and is subject to the following initial and boundary conditions:

$$\bar{T} = \bar{T}_i(\bar{r}) \quad \text{at} \quad \bar{z} = 0 \tag{3}$$

$$\text{for } \bar{z} > 0 \quad \bar{T} = T_w \quad \text{at} \quad \bar{r} = a \qquad \frac{\partial \bar{T}}{\partial \bar{r}} = 0 \quad \text{at} \quad \bar{r} = 0 \tag{4}$$

The last term in the energy equation is the viscous dissipation term, and it is always positive. This makes it clear that with the appearance of viscous heating, the symmetry of the solution with respect to heating and cooling[7] will be broken. Note that the inlet condition for temperature, Eq. (3), is a function of radial coordinate. A uniform inlet temperature distribution could be reasonably assumed for a simultaneously developing flow, one in which both the hydrodynamic and thermal fields are developing if $Pr >> 1$. The particular functional form of this initial condition is given by the solution for fully developed flow with viscous dissipation. For Newtonian flows ($n = 1$), $\bar{T}$ is a quartic function of $\bar{r}$. This initial condition will be given later in its dimensionless form.

### Dimensionless Core Formulation

In the core flow no boundary-layer behavior is experienced by the flow and the following dimensionless variables are introduced:

$$r_c = \bar{r}/a \quad \text{and} \quad z = \bar{z}/(a \cdot Pe) \tag{5}$$

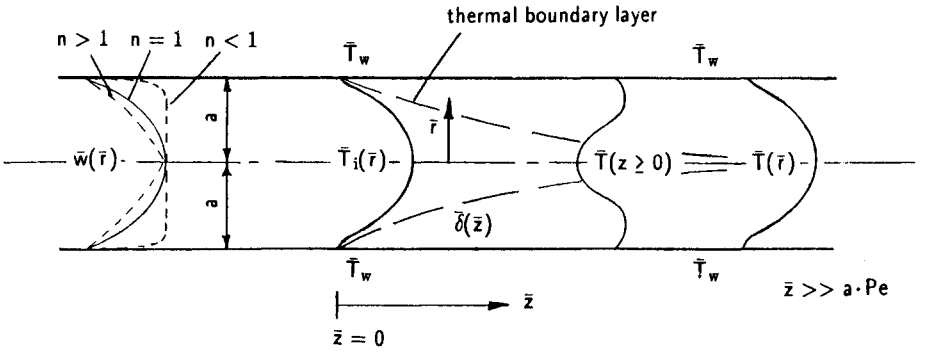


**Fig. 1 Physical model for thermally developing flows with viscous dissipation in an isothermal tube.**

$$w = \bar{w}/\bar{w}_{\max} \quad \text{and} \quad T = (\bar{T} - T_i^-)/(\bar{T}_w - T_i^-) \tag{6}$$

$T_i^-$ denotes the wall (minimum) temperature of the inlet distribution $\bar{T}_i(\bar{r})$ at $\bar{z} = 0$. At $\bar{z} \geq 0^+$, the wall temperature is $T_w$, which is distinctly different from $T_i^-$. Substitution of the dimensionless variables into the energy equation and its corresponding initial and boundary conditions results in

$$\left(\frac{3n+1}{n+1}\right)(1 - r_c^p)\frac{\partial T}{\partial z} = \frac{1}{r_c}\frac{\partial}{\partial r_c}\left(r_c\frac{\partial T}{\partial r_c}\right) + Br\left(\frac{3n+1}{n}\right)^{n+1} r_c^p \tag{7}$$

$$T = T_i(r_c) \equiv Br\left(\frac{3n+1}{n}\right)^{n-1}(1 - r_c^{3+1/n}) \quad \text{at} \quad z = 0 \tag{8}$$

$$\text{for } z > 0 \quad T = 1 \quad \text{at} \quad r_c = 1 \qquad \left(\frac{\partial T}{\partial r_c}\right) = 0 \quad \text{at} \quad r_c = 0 \tag{9}$$

A final condition ($z >> 1$) may also be deduced by inspection from the initial condition, Eq. (8). Because the only difference between the initial and final condition is the wall temperature, it follows that

$$T \rightarrow [1 + T_i(r_c)] \quad \text{as} \quad z \rightarrow \infty \tag{10}$$

**Dimensionless Boundary-Layer Formulation**

It has been pointed out previously[7] that the core formulation given previously is not a suitable model for the deep entry region. A new radial coordinate, designed to bring out the asymptotic, boundary-layer structure of this region must be used, namely

$$r = (a - \bar{r})/\bar{\delta}, \qquad r_c = 1 - r\delta, \qquad \delta = \bar{\delta}/a \tag{11}$$

Here, $\delta$ is the yet to be defined boundary-layer thickness; the boundary-layer thickness normalizes the dimensionless radial coordinate. Substitution of Eq. (11) into the core formulation, Eq. (7), leads to the boundary-layer equation

$$\left(\frac{3n+1}{n+1}\right)[1 - (1 - r\delta)^p]\left(\delta^2\frac{\partial T}{\partial z} - r\delta\delta'\frac{\partial T}{\partial r}\right) = \frac{\partial^2 T}{\partial r^2} - \left(\frac{\delta}{1 - r\delta}\right)\frac{\partial T}{\partial r} + \delta^2 Br\left(\frac{3n+1}{n}\right)^{n+1}(1 - r\delta)^p \tag{12}$$

which is subject to the following initial and boundary conditions:

$$T = T^+(r) \quad \text{at} \quad z = 0^+ \tag{13}$$

$$\text{for } z > 0^+ \quad T = 1 \quad \text{at} \quad r = 0$$
$$T \rightarrow r\delta Br[(3n+1)/n]^n\{1 - (r\delta/2)[(2n+1)/n] + \cdots\} \quad \text{as} \quad r \rightarrow \infty \tag{14}$$

The axial convection term in the core formulation is expanded into two terms through the use of the chain rule. The second of these terms has $\delta' = (d\delta/dz)$ as a coefficient. This coefficient incorporates the boundary-layer growth directly into the governing equation. Note that $r = 1$ when $\bar{r} = (a - \bar{\delta})$ for all $z$, i.e., the dimensionless domain of study is uniform. The far-field boundary condition ($r \rightarrow \infty$) in Eq. (14) has been obtained by substituting the boundary-layer coordinate, Eq. (11), into the initial condition, Eq. (8), and expanding the resulting expression in a power series about unity. This boundary condition has been presented in this way to more clearly show that it is inhomogeneous for all $z > 0^+$ (in which case $\delta > 0$).

The inhomogeneous nature of the far-field boundary condition causes a fundamental difficulty in determining an elementary solution for the initial condition, as well as in maintaining accuracy in the numerical solution. In order to circumvent this difficulty, it is advantageous to rewrite the formulation so that this boundary condition is homogeneous.

**Disturbance Temperature**

The key to being able to remove the far-field boundary condition inhomogeneity is to define a disturbance temperature $\tau(r, z)$, such that

$$T = T_i(r) + \tau \tag{15}$$

Here, $T_i(r)$ is the initial condition at the point $z = 0^-$. It may be obtained by substituting Eq. (11) into Eq. (8). Physically, $\tau(r, z)$ is the deviation of the temperature from its initially distributed or basic state. Substituting Eq. (15) into (12) and simplifying results in the disturbance energy equation for the boundary layer

$$\left(\frac{3n+1}{n+1}\right)[1 - (1 - r\delta)^p]\left(\delta^2\frac{\partial \tau}{\partial z} - r\delta\delta'\frac{\partial \tau}{\partial r}\right) = \frac{\partial^2 \tau}{\partial r^2} - \left(\frac{\delta}{1 - r\delta}\right)\frac{\partial \tau}{\partial r} \tag{16}$$

which is subject to the following initial and boundary conditions:

$$\tau = \tau^+(r) \quad \text{at} \quad z = 0^+ \tag{17}$$

$$\text{for } z > 0^+ \quad \tau = 1 \quad \text{at} \quad r = 0 \quad \text{and} \quad \tau \rightarrow 0 \quad \text{as} \quad r \rightarrow \infty \tag{18}$$

The far-field boundary condition, Eq. (18), is now homogeneous, in fact, the effect of viscous dissipation has completely vanished from the formulation. The solution for the disturbance temperature becomes simply the solution for the full boundary-layer temperature when there is no viscous dissipation. This startling result corroborates the earlier extended Lévêque solution by Shih and Tsou,[10] which indicated that viscous heating effects in the boundary layer are only of second-order. All that remains to complete the present formulation is to determine the nature of the initial condition $\tau^+(r)$, and to specify the boundary-layer thickness $\delta(z)$.

#### Asymptotic Solution

The initial condition $\tau^+(r)$ is the asymptotic solution of the disturbance temperature in the $Gz \rightarrow \infty$ ($z \rightarrow 0$) limit. In order to bring out the asymptotic structure of the disturbance energy equation for this limit, the $r_c^p$ terms in Eq. (12) are expanded into a power series in terms of $r$, $\delta$, and $p$ about the value of unity.[7] This series is substituted into the disturbance equation, Eq. (16), and then the limit $\delta \rightarrow 0$ (i.e., $Gz \rightarrow \infty$) is taken. The limiting form is

$$\frac{\partial^2\tau^+}{\partial r^2} + 3\lambda^3 r^2 \frac{\partial \tau^+}{\partial r} = 0 \quad \text{where} \quad \delta(z) = \left[\left(\frac{9\lambda^3 n}{3n+1}\right) z\right]^{1/3} \tag{19}$$

has been chosen for the boundary-layer thickness, a priori. This particular choice for $\delta$ collapses the partial differential equation (16) into the ordinary differential equation (19). Boundary conditions of Eq. (18) remain unchanged. The resulting solution for the initial condition

$$\tau^+ = 1 - 1.119847 \int_0^{\lambda r} \exp(-\mu^3)\, d\mu \tag{20}$$

is thus a similarity solution.[7] It may also be noted that the present asymptotic solution is exactly the zero-order solution of Shih and Tsou.

## Numerical Method

The formulation is solved using the numerical techniques developed in Prusa and Manglik.[7] The disturbance energy equation (16) is solved subject to the conditions specified in Eqs. (17), (18), and (20) for the boundary-layer region. The core energy equation (7) is solved subject to the boundary conditions specified in Eq. (9), and the initial condition given by the boundary-layer solution preceding it for the core region. As the boundary-layer scaling has eliminated the need to use very fine meshes or extremely accurate (high-order) finite difference methods, almost any standard technique may be used. Details of the finite differencing as well as the boundary layer to core matching may be found in Prusa and Manglik, and so are not repeated here. All of the numerical results presented in the following sections were generated using only 31 radial nodes, and approximately 2500 axial steps increasing in size monotonically with $z$ to go from the deep entrance region ($z = 10^{-6}$) to approximately fully developed flow (at $z = 3.0$). The accuracy of the resulting solutions has been amply demonstrated previously[7,16]; results so obtained for the classical Graetz problem were within 0.3% of the exact analytical solution.

## Results and Discussion

The results presented in the following sections are given in terms of both local and global distributions of dependent variables. The local results consist of detailed temperature distributions for two elementary cases: $n = 1$ (Newtonian fluid), and $Br = +1$ and $-1$ (heating and cooling, respectively). Global results are given in terms of bulk and centerline temperatures $Nu$ and an alternative heat transfer parameter $Q$. The bulk and centerline temperatures and $Nu$ results are shown only for the Newtonian cases. The local heat transfer rate in terms of the alternative parameter $Q$ are presented for the more generalized cases of power-law, non-Newtonian fluids ($n < 1$, pseudoplastics; and $n > 1$, dilatants), as well as for Newtonian fluids for $Br = \pm 1$, and compared with results from other studies in the literature.

Because variable axial step sizes were used in the computations, data is not generally available at a priori specified value of axial coordinate. Higher-order interpolations (second- through fourth-order, depending upon local axial resolution of results) are then used as needed to generate interpolated values accurate to at least three (and in most cases four) significant figures.

#### Temperature Distributions

The development of the radial temperature distribution is depicted in Fig. 2, in terms of a modified dimensionless temperature $T^*$. This temperature is based upon the definition given in Eq. (6), but modified to reflect the physical direction of the heat transfer:

$$T^* = \begin{cases} +T & \text{if} \quad Br \geq 0 \\ -T & \text{if} \quad Br < 0 \end{cases} \tag{21}$$

This change is required if cases with both heating and cooling are to be compared simultaneously. The horizontal coordinate is $(1 - r_c)$, which places the tube wall at zero and the tube center at unity. The initial condition for both cases ($n = 1$, and $Br = \pm 1$) is the same and is given by the middle of the three bold lines shown in the figure. The final condition for the heating case ($Br = +1$) is the upper of the three, whereas for the cooling case ($Br = -1$) it is the lowest of the three.

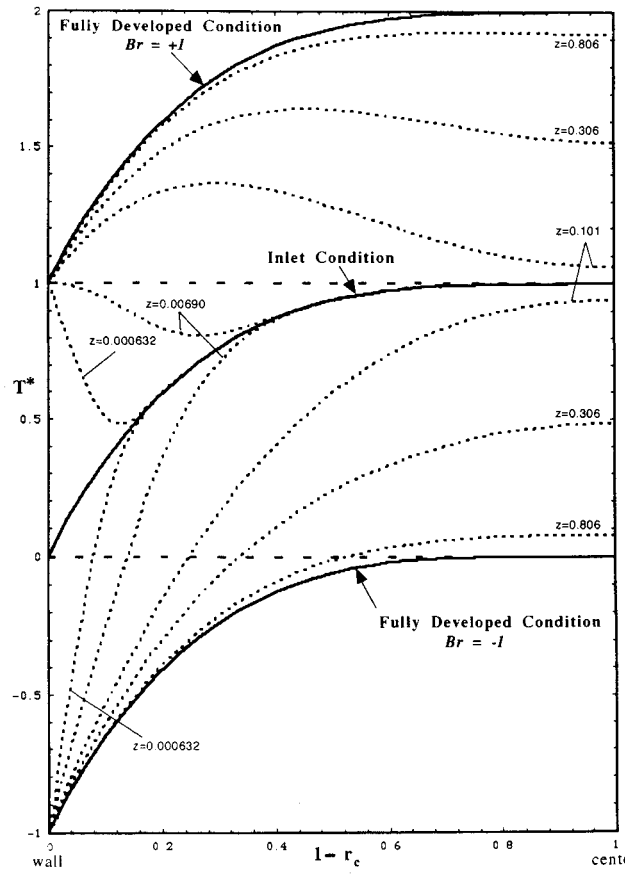


**Fig. 2 Axial development of the radial temperature distribution for the cases $n = 1$ and $Br = \pm 1$.**

For each case, five intermediate temperature distributions are also shown. The first, at $z = 0.000632$ lies in the deep entrance region, where the boundary-layer solution is valid. The disturbance temperature $\tau$ is clearly seen to be just that, a disturbance of the fully developed profile for viscous heating so that the wall boundary condition of $+1$ (heating case) or $-1$ (cooling case) may be met. The second distribution, at $z = 0.00690$, lies at the end of the boundary-layer regime. Although the boundary-layer thickness has more than doubled from $\delta = 0.22486$ (at $z = 0.000632$) to 0.49898 (at $z = 0.00690$) and the composite temperature, Eqs. (15) and (21), appears significantly different, the disturbance profile $\tau$ itself changes very little. In fact, throughout the boundary-layer region, $\tau$ is negligibly different from the initial distribution $\tau^+$ [given by the asymptotic solution, Eq. (20)]. The third distribution, at $z = 0.101$, shows the solution just beyond the boundary-layer regime. The centerline temperature now deviates noticeably from its initial value and the symmetry condition there has become important. The solution is now in a transition regime. This deviation of the centerline temperature from the initial condition has become most significant in the fourth distribution, at $z = 0.306$. The fifth intermediate distribution, at $z = 0.806$, shows the centerline temperature close to its fully developed value. The transition regime is drawing to an end and the solution is approaching its final, fully developed state.

The temperature field development shown in Fig. 2 is representative of all cases of $n$ and $Br$. A fundamental point is that the partition of the temperature into the inlet basic state and the boundary-layer disturbance temperature beautifully accounts for the sudden change in wall temperature that the fluid experiences.

#### Bulk and Centerline Temperatures

The bulk temperature is computed in the standard way using dimensional variables. Substitution of Eqs. (5) and (6) into the usual definition results in the dimensionless bulk temperature in terms of core variables, Eq. (22). In order to evaluate the bulk temperature in the boundary-layer region, Eq. (15) is first substituted into Eq. (22). The integral is then broken into its two constituent parts, a contribution from the basic state followed by a contribution from the disturbance temperature. The basic state term may be evaluated directly using Eq. (8). To determine the contribution from the disturbance temperature, the boundary-layer coordinate, Eq. (11), is substituted into the remaining integral. Since $\tau(r)$ is identically zero outside of the boundary layer, the integration limits for this integral are from zero (tube wall) to one (edge of the boundary layer); the final result is given by Eq. (23). One more expression for the bulk temperature may be obtained using the asymptotic solution $\tau^+(r)$ given by Eq. (20), and this is expressed in Eq. (24).

Core solution

$$T_m = \left(\frac{\bar{T}_m - T_i^-}{T_w - T_i^-}\right) = 2\left(\frac{3n+1}{n+1}\right)\int_0^1 (1 - r_c^p) T r_c \, dr_c \tag{22}$$

Boundary-layer solution

$$T_m = Br\left(\frac{4n+1}{5n+1}\right)\left(\frac{3n+1}{n}\right)^{n-1} + 2\left(\frac{3n+1}{n+1}\right) \times \int_0^1 [1 - (1 - r\delta)^p]\tau(1 - r\delta)\, dr \tag{23}$$

Asymptotic solution

$$T_m = Br\left(\frac{4n+1}{5n+1}\right)\left(\frac{3n+1}{n}\right)^{n-1} + 1.614601\left(\frac{3n+1}{n}\right)^{1/3} z^{1/3} \tag{24}$$

In both Eqs. (23) and (24), the first term on the right-hand side (RHS) is the contribution to the bulk temperature made by the basic state; the second term in each case is the contribution made by the disturbance temperature. The asymptotic formula, Eq. (24), is especially illuminating in that it shows that the contribution from the disturbance temperature (conduction effect in the boundary layer) vanishes as $Gz \to \infty$ ($\delta \to 0$), and that the basic state contribution dominates the bulk temperature throughout the boundary-layer region.

The numerical results for the axial development of the modified bulk and centerline temperatures is shown in Fig. 3; the results are for Newtonian flow ($n = 1$) with $Br = \pm 1$. The bulk temperature in the very deep entrance region, $z < 10^{-5}$, is constant and equal to (5/6) for both the heating and cooling cases. This value, set by the initial temperature distribution, has yet to be significantly influenced by the flow development [see Eq. (24)]. Effects of the boundary layer become dis-

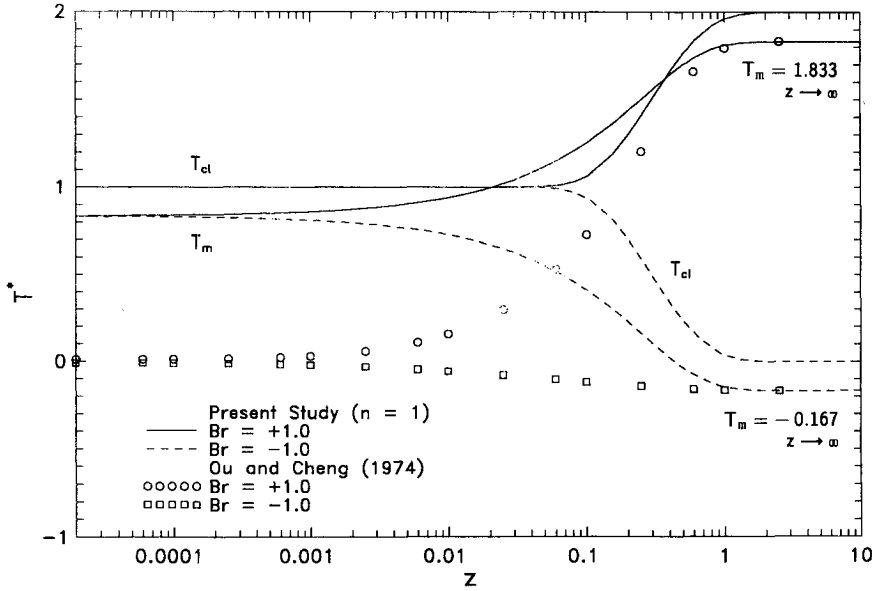


**Fig. 3 Axial development of the modified bulk and centerline temperatures for the cases $n = 1$ and $Br = \pm 1$.**

cernible in the figure by approximately $z = 10^{-4}$, and cause the bulk temperatures for the two cases to deviate from the initial value by 5% near $z = 0.0024$. However, the boundary-layer thickness becomes so wide at this point, $\delta = 0.35$, that the solution has very nearly reached the end of the boundary-layer region. Thus, the point at which the two bulk temperatures depart markedly from each other may be considered the beginning of the transition region. In the preceding boundary-layer region, the change in wall boundary condition is really not felt in terms of the bulk temperature. As $z$ continues to increase, the two bulk temperatures continue to grow further apart. Near $z = 0.77$, the two bulk temperatures have approached within 5% of their fully developed values, equal to $-1/6$ for $Br = -1$ and $11/6$ for $Br = +1$; the final state values of bulk temperatures may be obtained by adding one to the first term on the RHS of Eq. (24). This point may conveniently be considered to mark the end of the transition region and the beginning of the fully developed flow region. The numerical solutions are terminated at $z = 3.001$, at which point computations for bulk temperature lie within 0.17% of the exact fully developed flow values.

The numerical solutions for the centerline temperatures show a behavior that is qualitatively similar to that exhibited by the bulk temperature. The fundamental differences are that the centerline temperatures both start out with values of unity and have fully developed values of zero for $Br = -1$ and 2 for $Br = +1$. The centerline temperature may be seen to develop somewhat more slowly than the bulk temperature. This makes sense, as the effects of the change in wall temperature take longer to propagate to the center of the tube. Based upon the centerline temperature and the same 5% criterion as for the bulk temperature, the transition region is given by the axial interval $0.094 \leq z \leq 0.93$. While the beginning point is considerably later than that indicated by the bulk temperature, the endpoints are fairly similar in magnitude. A very interesting result suggested by Fig. 3 is that the bulk and centerline temperature profiles are symmetric with respect to $Br$ about their initial values. Detailed comparisons of the numerical results show that this is indeed correct to within 0.3%, which is the truncation error of the results. Because viscous dissipation causes a preferred direction for heat transfer (out of the fluid), this seems at first like an amazing result. It is, however, the direct result of Eq. (16), which gives the energy equation for the disturbance temperature. As noted earlier, this equation has the remarkable property that it is free of any $Br$ dependence. Thermal development, that is driven by a change in wall temperature, affects cooling cases the same as heating cases, despite the preferential direction of heat transfer due to viscous dissipation.

Finally, Fig. 3 shows additional analytical results for bulk temperature from Ou and Cheng.[3] These results, which are for the case of uniform inlet temperature (a value of zero for the dimensionless temperature used for the figure), provide an excellent complement to the present results. They show the same qualitative trends and are in very good agreement with the present results as to the extent of the transition region. The Ou and Cheng[3] results converge to the same final states as the present results as $z \to \infty$; $T^* = -r^4$ for $Br = -1$ and $T^* = (2 - r^4)$ for $Br = +1$. Since the uniform temperature initial condition is a reasonable approximation for simultaneously developing high $Pr$ flows, all possible initial states will result in solutions that lie in-between the present results and those of Ou and Cheng.

### Nusselt Number

The usual tube diameter-based definition of local Nusselt number is employed. As for the case of bulk temperature, $Nu$ is computed in terms of both core and boundary-layer variables. A third expression is computed in terms of the asymptotic boundary-layer solution ($\tau^+$). It has value in that it enhances the physical interpretation of the effect of the boundary layer in the deep entrance region. A fourth expression gives the final, fully developed value of $Nu$. These expressions are as follows:

Core solution

$$Nu = \left[\frac{2}{(1 - T_m)}\right]\left(\frac{\partial T}{\partial r_c}\right)_1 \tag{25}$$

Boundary-layer solution

$$Nu = -\left(\frac{2}{1 - T_m}\right)\left[Br\left(\frac{3n + 1}{n}\right)^n + \frac{1}{\delta}\frac{\partial \tau}{\partial r}\bigg|_0\right] \tag{26}$$

Asymptotic solution

$$Nu = [2/(1 - T_m)]\{-Br[(3n + 1)/n]^n + 1.119847[9nz/(3n + 1)]^{-1/3}\} \tag{27}$$

Final state

$$Nu \to Nu_\infty = 2\left(\frac{3n + 1}{n}\right)\left(\frac{1 + 5n}{1 + 4n}\right) \quad \text{as} \quad z \to \infty \tag{28}$$

The first terms in the brackets in Eqs. (26) and (27) represent the contributions to $Nu$ from the basic state profile; the second terms represent the boundary-layer disturbance contributions. The asymptotic formula, Eq. (27), is very revealing in that it shows that the disturbance gradient overwhelms the basic state gradient as $Gz \to \infty$ ($z \to 0$). Unlike the case of zero dissipation, however, the basic state profile still has a strong effect on the value of $Nu$ through its influence on the bulk temperature. The final expression for $Nu$, Eq. (28), is noteworthy because it has no $Br$ dependency, despite the fact that the wall temperature gradient does show such dependency.

Figure 4 shows the effects of viscous dissipation on the axial development of the local $Nu$ as defined by Eqs. (25) and (26). Present numerical results for $Br = \pm 1$ are depicted over the complete axial range from the deep entry region to fully developed flow. Asymptotic results for smaller values of $z$ are shown using Eq. (27). Additional results from Ou and Cheng,[3] and Shih and Tsou[10] are also plotted. The present asymptotic solution faithfully replicates the numerical results with increasing fidelity as $z \to 0$. It follows the numerical result extremely closely, and lies within 1.3% of it for $z \leq 10^{-5}$, and within 5% for $z \leq 10^{-3}$ for the case $Br = -1$. For the case $Br = +1$ the asymptotic result lies within 1.6% of the numerical result for $z \leq 10^{-5}$, and within 18% for $z \leq 10^{-3}$ (a 5% deviation occurs at $z = 0.000133$). The Shih and Tsou results appear to match the present results reasonably well only in the transition region. For smaller values of $z$, (deeper in the entry region), they are skewed by the different bulk temperature of the initial state. Actually, the effect of the initial condition is still quite strong in the transition region, and it forces $Nu$ to remain significantly larger than the values predicted with the present initial condition. At the closest, they are some 30% larger in magnitude at $z = 0.00525$. For larger values of $z$, the Shih and Tsou $Nu$ diverges even more, because it is computed from an extended Lévêque solution that is not valid for large $z$. At $z = 0.101$, the $Nu$ of Shih and Tsou diverges from the present results by 66%.

The Ou and Cheng solutions for $Nu$ match the present solutions extremely closely, within 0.26%, in the fully developed flow region. In the transition and boundary-layer regions, they diverge from the present results due to the different initial condition and the classical Graetz function expansion, respectively. In the transition region the Ou and

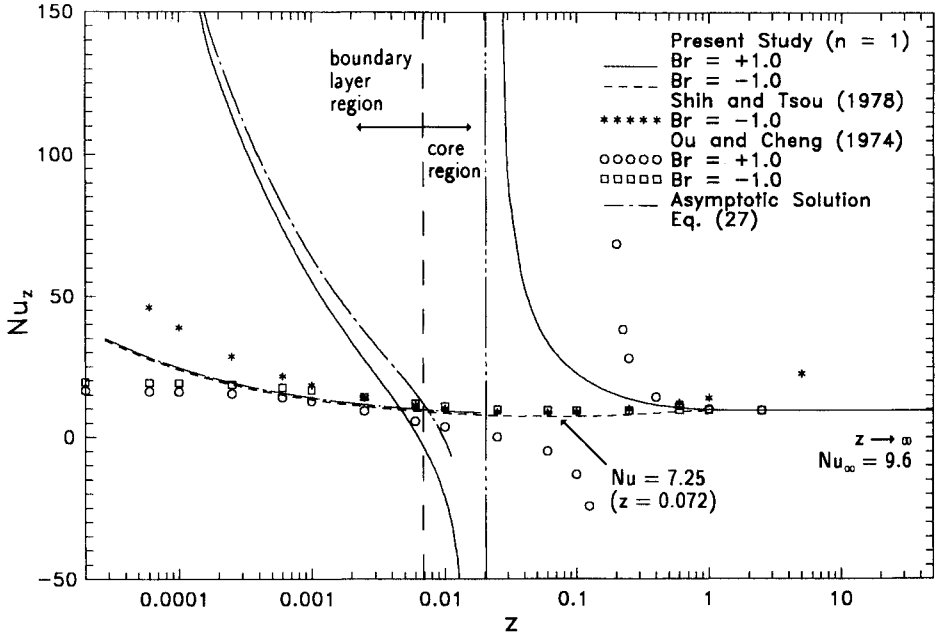


**Fig. 4 Axial development of the local Nusselt number $Nu_z$ for the cases $n = 1$ and $Br = \pm 1$.**

Cheng results match the Shih and Tsou results very well. These two solutions for $Nu$ lie within 1% of each other in the axial interval $0.0029 \leq z \leq 0.00707$. Deeper in the entrance region, however, the Ou and Cheng results diverge from the Shih and Tsou results by 8% or more for $z < 0.001$ and by 48% or more for $z < 0.0001$. This divergence is due to the nonuniform convergence of the Graetz series solution. In Prusa and Manglik,[7] it is pointed out that even the first 121 terms of the series are insufficient for accurate predictions of $Nu$ when $z \leq 0.0004$. Finally, for larger values of $z$, the Shih and Tsou solution diverges from the Ou and Cheng solution by 23% or more for $z > 0.100$. This is considerably less than the divergence with respect to the present solution, and indicates that the value of the local $Nu$ is still sensitive to the initial condition at this axial location.

Comparisons aside, Fig. 4 looks puzzling and one is tempted to believe something is wrong. The results appear nonsensical, yet they are extremely accurate. The $Nu$ behavior for the case $Br = -1$ seems almost reasonable. The only notable trait is the existence of a local minimum value of 7.25 at $z = 0.0720$. But the results for the case $Br = +1$ show $Nu$ decreasing from $+\infty$ at $z = 0^+$, to a value of zero at $z = 0.00631$, to a value of $-\infty$ at $z = 0.0209$. The point discontinuity in $Nu$ at $z = 0.0209$ is due to the bulk temperature passing through the value of the wall temperature there (in dimensionless form $T_m \rightarrow 1$). Thus, the coefficient of the temperature gradient in Eqs. (25) and (26) becomes unbounded, going to $-\infty$ when $T_m \rightarrow 1$ from below (small $z$ side, Fig. 3), and going to $+\infty$ when $T_m \rightarrow 1$ from above (large $z$ side). More generally, for heating cases ($Br > 0$), the bulk temperature will increase with axial coordinate. Whenever the initial bulk temperature is less than the wall temperature, the potential exists that at some nonzero value of $z$ the bulk temperature will become equal to the wall temperature, and $Nu$ will become discontinuous there. Note that the Ou and Cheng solution for $Br = +1$ also shows this same type of point discontinuity in the axial development of $Nu$, only it occurs somewhat later at $z = 0.174$ (where $\bar{T}_m = T_w$), due to the somewhat different development history of the bulk temperature (Fig. 3). The same type of discontinuity may occur in cooling cases ($Br < 0$). If the initial bulk temperature is greater than the wall temperature, then the potential exists that as the bulk temperature decreases with increasing $z$, it may at some point equal the wall temperature. Whether or not the dimensionless bulk temperature attains a value of unity depends upon the respective magnitudes of $Br$ and $n$.

The modified bulk temperature for the initial condition, $T^*_{m,i}$, given by the first term on the RHS of Eqs. (23) and (24) in conjunction with Eq. (21), is helpful in seeing under what conditions this discontinuity may occur. This equation is plotted as a contour map in the ($n$, $Br^*$) plane in Fig. 5, Here, $Br^*$ is a modified Brinkman number, equal to $+Br$ if $Br > 0$ and $-Br$ if $Br < 0$. For heating cases, if $T^*_{m,i} < 1$, then a $Nu$ discontinuity may occur at some nonzero value of $z$. For cooling cases also, if $T^*_{m,i} > 1$, then a $Nu$ discontinuity may occur. While $Nu$ behaves in this most peculiar fashion, it will be shown in the following section that the temperature gradient at the wall, and hence, the heat transfer rate, behaves in a most orderly and physically sensible fashion. Also recall that the fully developed value of $Nu$ given by Eq. (28) is not a function of $Br$, whereas the actual convection heat transfer rate at the wall is a function of $Br$. Clearly the conventional $Nu$ is not a meaningful measure of the heat transfer rate in this case. The next section will show the same heat transfer results (plus additional results for non-Newtonian flows), but using a more general measure of the convection heat transfer rate.

### Heat Transfer Revisited

A more appropriate measure of the convection heat transfer rate, one that faithfully follows the heat flux at the wall, must depend only upon the wall temperature gradient. It is the dependency of $Nu$ upon the bulk temperature that is responsible for its failure to behave in a physically meaningful way. Another requirement for a more reasonable convection heat transfer parameter is that it should be sign preserving. Because the effect of dissipation is always to add thermal energy to the fluid, it makes a difference whether or not the wall temperature change induces heating ($\Delta T_i$, $Br > 0$) or cooling ($\Delta T_i$, $Br < 0$). From these considerations, a suitable dimensionless heat transfer rate may be defined as

$$Q = \frac{qa}{k|\Delta T_i|} = \begin{cases} +\left(\dfrac{\partial T}{\partial r_c}\right)_1 & \text{if} \quad Br \geq 0 \\ -\left(\dfrac{\partial T}{\partial r_c}\right)_1 & \text{if} \quad Br < 0 \end{cases} \tag{29}$$

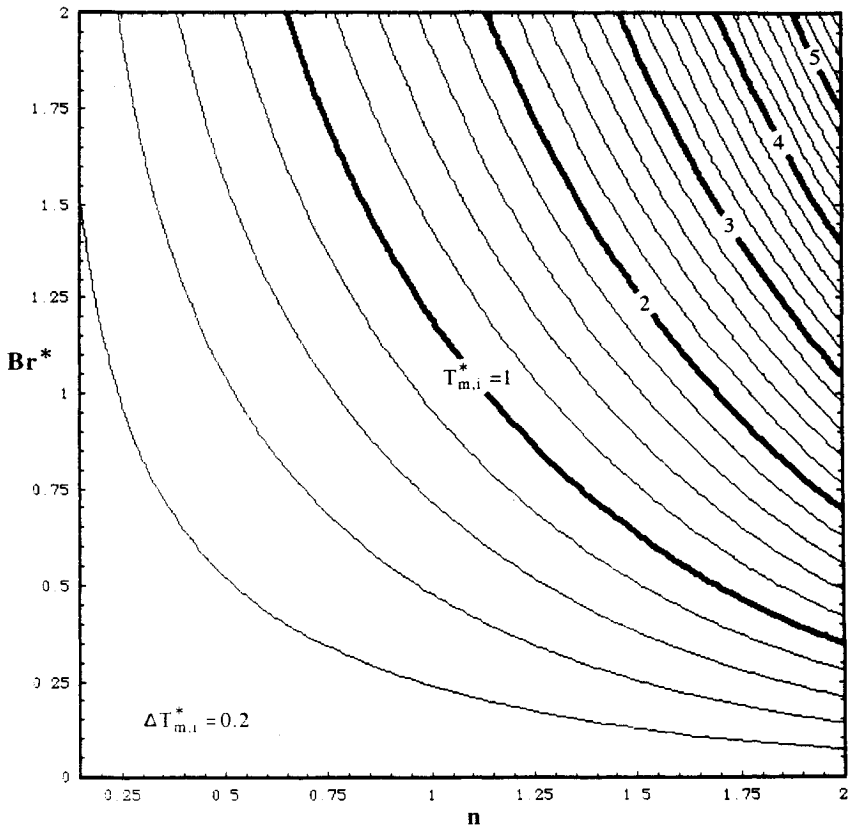


**Fig. 5 Lines of constant bulk temperature for the basic state (inlet condition) as a function of $n$ and $Br$.**

Here, $q$ refers to the local dimensional heat flux rate at the tube wall, and it may be positive (heating) as well as negative (cooling). The sign convention for $q$ is that $q < 0$ if the direction of heat transfer is from the fluid to the surroundings. The use of the absolute value of the temperature change forces the dimensionless heat transfer rate $Q$ to have the same sign as $q$; the plus or minus signs in Eq. (29) provide this sense of direction, given the nondimensionalization. While Eq. (29) gives $Q$ only in terms of the core coordinates, it may easily be converted into the boundary-layer coordinates or asymptotic form; the conversions may be found at once from inspection of Eqs. (25–27).

It may be noted that $Q$ given by Eq. (29) can be readily calculated for most practical heat exchangers. The constant wall temperature boundary simulates the condition when phase change (steam condensation or refrigerant evaporation) or turbulent flow of high heat capacity fluids occurs on the outside of the tube. In these cases, the shellside convective resistance and metallic tube wall resistance are negligibly small in comparison with the laminar in-tube flows of viscous liquids. Thus, the tube wall temperature, to a good first approximation, is almost the same as the shellside bulk fluid temperature, and hence, $\Delta T_i$ can be calculated. Second-order refinements can easily be made through a simple iterative procedure, very similar to that for estimating the bulk-to-wall temperature viscosity ratio in most heat exchanger calculations.

Figure 6 shows the axial development of $Q$ for six separate cases, $Br = \pm 1$, and $n = 0.5$, 1, and 2. In each case, $Q$ decreases from $\pm\infty$ at $z = 0^+$ (according to whether or not $Br > 0$ or $< 0$), like $\pm z^{-1/3}$ as $z \to 0^+$. As the temperature field becomes fully developed ($z \to \infty$), for a given value of flow behavior index $n$, the two development curves for $Q$ corresponding to $Br = \pm 1$ converge to a common value $Q_\infty$. This fully developed value of $Q$ is given by the first term on the RHS of Eqs. (26) or (27), with the modified Brinkman number $Br^*$ as defined in the preceding subsection being used in place of $Br$. This convergence makes sense, because the final states depend only upon the magnitude of $Br$ and not at all upon its sign. Unlike the earlier $Nu$ plot, there are no puzzling asymptotes in the figure for nonzero values of $z$ where $Q$ becomes unbounded.

Additional inspection of Fig. 6 reveals that the wall temperature gradient generally increases with decreases in the value of flow behavior index $n$, for given values of $Br$ and $z$. This parallels the result for non-Newtonian flows without viscous dissipation.[7] Careful examination reveals that exceptions to this general trend do occur. In particular, for the case $n = 0.5$ and $Br = -1$, it may be seen that $Q$ lies below the corresponding result for the case $n = 1$ and $Br = -1$ in the deep entrance region. At $z = 0.0000445$, the two development histories cross, and the $n = 0.5$ plot assumes the more general trend of lying above the $n = 1$ plot for all larger values of $z$. This behavior may be explained by turning to the asymptotic solution, Eqs. (29) circa (27), which can actually be used to generate the locations of these crossover points as long as they lie deep in the entrance region [so that Eq. (27) is a valid approximation]. Equation (27) reveals that, in the boundary-layer region, the flow behavior index affects the wall temperature gradient through two terms: one due to the dissipation effects of the initial state, and the other due to boundary-layer growth. When $Br > 0$, these two terms have opposite signs, and hence, affect the wall gradient in opposite fashion.

Wall temperature gradient results from the studies of Ou and Cheng,[3] and Shih and Tsou[10] are also presented in Fig. 6. As was the case with the axial development of $Nu$, in the fully developed region the Ou and Cheng results for $n = 1$ and $Br = \pm 1$ match the present results extremely well. The difference, 0.3%, is the truncation error of the present results. As $z$ decreases into the transition region, the Ou and Cheng results diverge from the present results primarily due to the different initial condition being used. For the case $Br = +1$, this divergence exceeds 5% for $z \leq 0.527$, and exceeds 10%

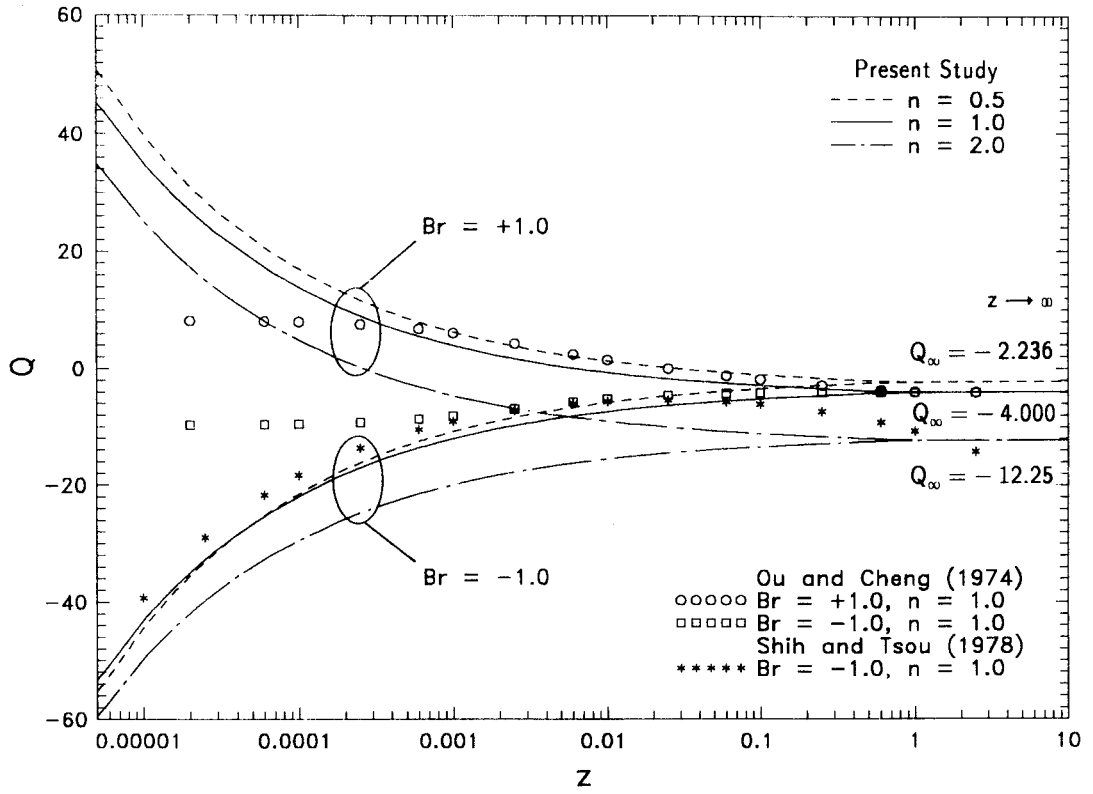


**Fig. 6 Axial development of the dimensionless local convection heat transfer rate $Q$ for the cases $n = 0.5$, 1.0, and 2.0, and $Br = \pm 1$.**

for $z \leq 0.358$; for the case $Br = -1$, the corresponding values are $z = 0.497$ and 0.299. For still smaller values of the axial coordinate, the Ou and Cheng results fail to increase in magnitude due to the limited number of terms being used in the Graetz series solution. Unlike the *Nu* behavior (Fig. 4) discussed earlier, the wall temperature gradient predicted by Shih and Tsou for the case $Br = -1$ matches the present solution considerably better over the entire deep entrance region. This matching improves as $z \rightarrow 0^+$, a behavior that may be understood by examining Eqs. (29) circa (27), where it can be seen that in the deep entry region all effects of dissipation vanish. Thus, the effect of the initial condition upon the wall temperature gradient decreases as the thermal entrance point is approached, and the solution of Shih and Tsou becomes indistinguishable from the present one. The two results lie within 10% of each other for $z \leq 1.51 \times 10^{-5}$. This difference is due to the uniform initial condition. That the difference is this large so deep in the entry region is somewhat surprising given the asymptotic solution, Eqs. (29)/(27), for the wall gradient and the result from Shih and Tsou that dissipation effects are of the second-order in the boundary-layer region. The present asymptotic result for the case $Br = -1$ converges much faster to the present numerical result and lies within 10% of it as far downstream as $z \leq 0.0122$; for $z \leq 4.95 \times 10^{-6}$, it lies within 1% of the present numerical result. Ultimately the Shih and Tsou results do converge to the present ones, for $z \leq 6.71 \times 10^{-9}$ they lie within 1% of each other.

## Summary and Conclusions

This study has successfully generalized a numerical method based upon an asymptotic analysis of the deep entrance region of a thermally developing flow with viscous dissipation. This generalization required the decomposition of the temperature field into a basic state (inlet condition) and a disturbed state in order to generate the homogeneous initial condition that the asymptotic solution requires. A startling result of this decomposition is the finding that viscous dissipation effects on the wall temperature gradient vanish in the boundary layer as $z \rightarrow 0^+$. The results presented in this work are based upon a nonuniform inlet condition in which dissipation effects are already fully present. This contrasts with and complements earlier studies in the literature for which a uniform inlet condition is generally assumed (approximately corresponding to the inlet condition for simultaneously developing, high *Pr* flows).

The present study's reliance upon the asymptotic scales of the deep entrance region has allowed very accurate results to be generated from a location (arbitrarily) deep in the entrance region all the way to the fully developed flow region. This accuracy has clearly revealed several interesting and fundamental behaviors in the axial development of the Nusselt number and wall temperature gradient. Three distinct characteristics have been noted:

1) The wall temperature gradient generally increases with decreases in the value of the flow behavior index $n$. As $n$ decreases, the velocity profile becomes more uniform with correspondingly larger wall gradients. This parallels the behavior for non-Newtonian, power-law fluid flows without dissipation.

2) For heating conditions, a more complex behavior for wall gradient is possible deep in the boundary layer. In particular, the initial wall gradient will increase with $n$. This behavior is due solely to viscous dissipation and is opposite to the usual behavior of a nondissipative power-law fluid. At some small value of $z$ a crossover will occur and the behavior will switch to that noted in 1.

3) The Nusselt number has been observed to correlate poorly with the wall temperature gradient. Physically this occurs because the bulk temperature axial development is nontrivial. Where it becomes equal to the wall temperature, *Nu* becomes unbounded. In effect, *Nu* breaks down as a measure of the convection heat transfer rate due to the intrinsic nonlinearity of the relationship between the convection heat transfer coefficient and the heat transfer rate.

## Acknowledgment

The authors would like to thank the National Center for Atmospheric Research, Boulder, Colorado, for the computing resources for this work.

## References

[1]Brinkman, H. C., "Heat Effects in Capillary Flow I," *Applied Science Research*, Vol. A2, No. 2, 1951, pp. 120–124.

[2]Toor, H. L., "Heat Transfer in Forced Convection with Internal Heat Generation," *AIChE Journal*, Vol. 4, No. 3, 1958, pp. 319–323.

[3]Ou, J.-W., and Cheng, K. C., "Viscous Dissipation Effects on Thermal Entrance Heat Transfer in Laminar and Turbulent Pipe Flows with Uniform Wall Temperature," American Society of Mechanical Engineers Paper 74-HT-50, 1974; also AIAA Paper 74-743, July 1974.

[4]Krishnan, K. N., and Sastri, V. M. K., "Numerical Solution of Thermal Entry Length Problem with Variable Viscosities and Viscous Dissipation," *Wärme- und Stoffübertragung*, Vol. 11, No. 2, 1978, pp. 73–79.

[5]Lawal, A., and Mujumdar, A. S., "Extended Graetz Problem—A Comparison of Various Solution Techniques," *Chemical Engineering Communications*, Vol. 39, Nos. 1–6, 1985, pp. 91–100.

[6]Shah, R. K., and London, A. L., *Laminar Flow Forced Convection in Ducts, Supplement 1 to Advances in Heat Transfer*, Academic, New York, 1978.

[7]Prusa, J., and Manglik, R. M., "Asymptotic and Numerical Solutions for Thermally Developing Flows of Newtonian and Non-Newtonian Fluids in Circular Tubes with Uniform Wall Temperature," *Numerical Heat Transfer*, Pt. A, Vol. 26, No. 2, 1994, pp. 199–217.

[8]Lévêque, M. A., "Les Lois de la Transmission de Chaleur par Convection," *Annales des Mines, Memoires*, Series 12, Vol. 13, March 1928, pp. 201–299, 305–362, 381–415.

[9]Gill, W. N., "Heat Transfer in Laminar Power Law Flow with Energy Sources," *AIChE Journal*, Vol. 8, No. 1, 1962, pp. 137, 138.

[10]Shih, Y.-P., and Tsou, J.-D., "Extended Leveque Solutions for Heat Transfer to Power Law Fluids in Laminar Flow in a Pipe," *Chemical Engineering Journal*, Vol. 15, No. 1, 1978, pp. 55–62.

[11]Richardson, S. M., "Extended Leveque Solutions for Flows of Power Law Fluids in Pipes and Channels," *International Journal of Heat and Mass Transfer*, Vol. 22, No. 10, 1979, pp. 1417–1423.

[12]Gottifredi, J. C., and Flores, A. F., "Extended Leveque Solution for Heat Transfer to Non-Newtonian Fluids in Pipes and Flat Ducts," *International Journal of Heat and Mass Transfer*, Vol. 28, No. 5, 1985, pp. 903–908.

[13]Gryglaszewski, P., Mowak, Z., and Stacharska-Targosz, J., "The Effect of Viscous Dissipation on Laminar Heat Transfer for Power Law Fluids in Tubes," *Wärme- und Stoffübertragung*, Vol. 14, No. 2, 1980, pp. 81–89.

[14]Lawal, A., and Mujumdar, A. S., "The Effects of Viscous Dissipation on Heat Transfer to Power Law Fluids in Arbitrary Cross-Sectional Ducts," *Wärme- und Stoffübertragung*, Vol. 27, No. 7, 1992, pp. 437–446.

[15]Bird, R. B., Stewart, W. E., and Lightfoot, E. N., *Transport Phenomena*, Wiley, New York, 1960.

[16]Manglik, R. M., and Prusa, J., "An Improved Solution Based on Asymptotic Analysis and Numerical Methods for the Graetz Problem," Dept. of Mechanical Engineering, Rept. ISU-ERI-Ames-88117, Iowa State Univ., Ames, IA, Oct. 1987.